Efficient Augmented Lagrangian Formulation for the Combined Simulation of Multibody and Hydraulic Dynamics

Javier Cuadrado, Miguel A. Naya
Laboratory of Mechanical Engineering
University of La Coruña
Ferrol, 15403, Spain
Email: {javicuad,minaya}@cdf.udc.es

Daniel Dopico, Urbano Lugris
Laboratory of Mechanical Engineering
University of La Coruña
Ferrol, 15403, Spain
Email: {ddopico,ulugris}@udc.es

Several years ago, the authors proposed a method for the efficient simulation of the dynamics of multibody systems: the modeling of the system was carried out in natural or fully-Cartesian coordinates (dependent and absolute coordinates), the equations of motion were stated as an index-3 augmented Lagrangian formulation, the numerical integration was performed through Newmark-type algorithms, and the resulting velocities and accelerations were projected into their corresponding constraint manifolds. The formalism showed to be robust and efficient: it worked properly in mechanisms with singular configurations or changing topologies, and provided successful results for large and complex industrial problems, like the detailed models of cars and excavators. Some years later, the method was extended so as to consider the modeling in joint coordinates (dependent and relative coordinates), taking advantage of the recursive kinematics and dynamics allowed for such an approach, which led to a method with improved efficiency for large systems.

Hydraulic actuators play a relevant role in many industrial fields, like heavy machinery, aircraft or entertainment. A common simplified technique to include the behaviour of hydraulic actuators within simulations of multibody dynamics consists of kinematically guide the variable length corresponding to the distance between the ends of the hydraulic actuator. The guidance law which provides the actuator length as function of the driving inputs (provided by, let's say, the machine operator) may be just a linear mapping or may account for force or speed limitations and other characteristics of the real power system.

However, a more detailed modeling is required when the hydraulic dynamics of the actuators should be taken into account. This can be done through linearized or fully nonlinear differential equations, depending on the level of detail required in the solution. When addressing the nonlinear approach (pressures in the hydraulic chambers are coupled with the system motion), two different methods have been followed. The first one combines the hydraulic and multibody dynamic equations, thus yielding a unified system of differential equations which is integrated in time by means of a single integration scheme. The second one applies co-simulation, so that each problem is separately solved by means of a different integration scheme, and information is exchanged between the two processes: typically, the multibody problem leads the solution process, since its lower stiffness allows for larger time-step sizes.

In this work, the first method is applied: both the hydraulic and multibody dynamic equations are combined within the formalism described in the first paragraph in a unified approach. The resulting formalism is developed, and the raised numerical issues are discussed. An academic example serves to compare the complexity and efficiency of the simplified (kinematic guidance) and detailed approaches (fully nonlinear differential equations), leading to conclude that the robustness of the unified method is preserved and that the efficiency of the method is only moderately penalized.

EFFICIENT AUGMENTED LAGRANGIAN FORMULATION FOR THE COMBINED SIMULATION OF MULTIBODY AND HYDRAULIC DYNAMICS

Javier Cuadrado, Miguel A. Naya
Laboratory of Mechanical Engineering
University of La Coruña
Ferrol, 15403, Spain
Email: {javicuad,minaya}@cdf.udc.es

Daniel Dopico, Urbano Lugris
Laboratory of Mechanical Engineering
University of La Coruña
Ferrol, 15403, Spain
Email: {ddopico,ulugris}@udc.es

ABSTRACT

Several years ago, the authors proposed a method for the efficient simulation of the dynamics of multibody systems: an index-3 augmented Lagrangian formulation with projections in velocities and accelerations to the constraint manifold, which relied on Newmark-type algorithms for the numerical integration in time. The formalism showed to be robust and efficient when facing a number of large and complex problems, as the detailed models of cars and excavators.

On the other hand, hydraulic actuators are present in many industrial applications of multibody dynamics techniques, like in the case of the heavy machinery field. When simulating the dynamics of this kind of problems, two different approaches are common: to resort to kinematically guide the variable length of the actuator, thus avoiding the need to consider the dynamics of the hydraulic system; or to perform a multi-rate integration of both phenomena if a more detailed description of the problem is required, for example, when the objective of the study is to optimize the pump control.

This work addresses the inclusion of hydraulic actuators dynamics in the method for the simulation of multibody system dynamics mentioned above. The resulting formalism is developed, and the raised numerical issues are discussed. An academic example serves to compare the complexity and efficiency of the simplified (kinematic guidance), multi-rate and unified approaches, leading to conclude that the robustness of the method is preserved and that the efficiency of the method is moderately penalized.

Keywords: multibody dynamics, hydraulic dynamics, augmented Lagrangian formulation, efficient simulation, hydraulic cylinders, heavy machinery.

1. INTRODUCTION

Several years ago, the authors proposed a method for the efficient simulation of the dynamics of multibody systems [1]: the modeling of the system was carried out in natural or fully-Cartesian coordinates (dependent and absolute coordinates), the equations of motion were stated as an index-3 augmented Lagrangian formulation, the numerical integration was performed through Newmark-type algorithms, and the resulting velocities and accelerations were projected into their corresponding constraint manifolds. The formalism showed to be robust and efficient: it worked properly in mechanisms with singular configurations or changing topologies, and provided successful results for large and complex industrial problems, like the detailed models of cars and excavators, allowing integration time steps as large as 10 ms. Some years later, the method was extended [2] so as to consider the modeling in joint coordinates (dependent and relative coordinates), taking advantage of the recursive kinematics and dynamics allowed for such an approach, which led to a method with improved efficiency for large systems.
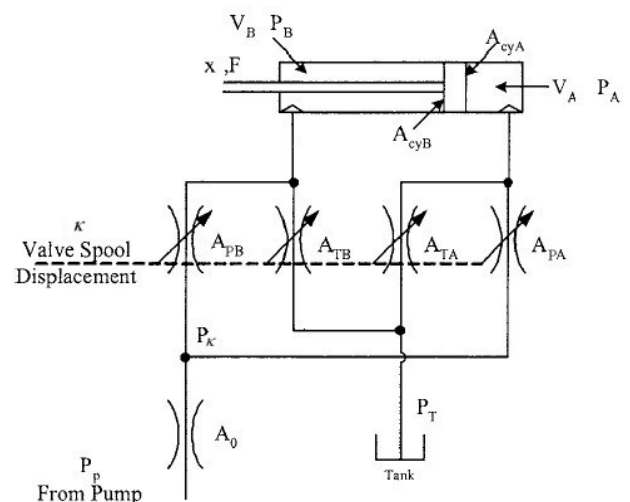

Figure 1: DIAGRAM OF A HYDRAULIC CYLINDER AND VALVE.

Hydraulic actuators play a relevant role in many industrial fields, like for example in most heavy machinery systems [3, 4]. The dynamics of such devices are usually

modeled in terms of the orifice equations, volumes and pressure areas, as depicted in Fig. 1. Pressure rates for the volumes on both sides of the cylinder piston are derived from fluid continuity and compressibility concepts [5] as

$$\dot{p}_A = \frac{\beta_A}{V_A}\left(-\dot{V}_A + Q_{PA} + Q_{TA} + Q_{BA}\right) \qquad (1)$$

$$\dot{p}_B = \frac{\beta_B}{V_B}\left(-\dot{V}_B + Q_{PB} + Q_{TB} + Q_{BA}\right) \qquad (2)$$

where Q_{BA} represents the leakage flow and is commonly neglected. The bulk modulus at each side of the cylinder, β_i, is obtained as function of the pressures as

$$\beta_i = \frac{1 + ap_i + bp_i^2}{a + 2bp_i} \qquad (3)$$

with a and b being known constants for the fluid. The flow across each orifice area, A_{orf}, in a hydraulic valve is given by

$$Q = A_{orf}C_d\sqrt{\frac{2\left(p_{in} - p_{out}\right)}{\rho}}sign\left(p_{in} - p_{out}\right) \qquad (4)$$

being p_{in} and p_{out} the pressures at both sides of the orifice.

In the valve, there are four orifice areas which are a nonlinear function of the spool displacement, κ, corresponding to $A_{PA}\left(\kappa\right)$, $A_{TA}\left(\kappa\right)$, $A_{PB}\left(\kappa\right)$, $A_{TB}\left(\kappa\right)$. The displacement of the spool includes some dead zones to minimize leakage [6]. The variation of the pressure provided by the pump is a nonlinear function of the speed, the flow, the leakages and the geometry of the pump, but this is not taken into account in this work.

A common simplified technique to include the behavior of hydraulic actuators within simulations of multibody dynamics consists of kinematically guide the variable length corresponding to the distance between the ends of the hydraulic actuator [7]. The guidance law which provides the actuator length as function of the driving inputs (provided by, let's say, the machine operator) may be just a linear mapping or may account for force or speed limitations and other characteristics of the real power system.

However, for some applications, e.g. when optimization of the pump control is sought, a more detailed modeling is required, and the dynamics of hydraulic actuators should be taken into account. Some attempts have been presented in the literature in this direction [8, 9]. From

the integration point of view, two different approaches have been followed, namely, the unified approach, and the co-integration.

The first one combines the hydraulic and multibody equations, thus yielding a single system [10, 11] that is then integrated in time.

In the second approach, one problem leads the solution process and, usually, its integration time-step size is larger. Therefore, both problems are integrated separately, but information is exchanged between them at every integration time step of the main process. This is known as multi-rate integration, and can be carried out by either employing a different software for each problem (co-simulation) [9, 12] or a single environment where both problems are integrated separately (co-integration) [13,14]. Hydraulic devices are easily modeled by a few first-order nonlinear differential equations, but it is a numerically stiff set of equations due to the high "stiffness" of the hydraulic fluid, which is characterized by a bulk modulus that may raise to 700 MPa. This problem may be overcome by using a very small time-step size for the integration that ranges typically between 10^{-6} s and 10^{-4} s [15]. Consequently, the multibody integration leads the process and the hydraulic problem is solved with a smaller time-step size.

In this work, the first approach from those that take the hydraulic dynamics into account is addressed: both hydraulic and multibody dynamic equations are combined within the formalism mentioned at the beginning of the Section in a unified approach. The efficiency of this scheme is tested by comparison with the kinematic guidance of hydraulic actuators. The accuracy of the solution is contrasted with that of a co-integration scheme. The organization of the paper is as follows: the original method for multibody dynamics is briefly exposed in Section 2; the inclusion of the hydraulic dynamic equations is addressed in Section 3, and the resulting formalism is obtained; an academic example aimed to test the behavior of the proposed scheme is presented in Section 4, while in Section 5 the results coming from the simulation of the example are discussed and compared with those of the other approaches mentioned above; finally, the conclusions are summarized in Section 6.

2. THE ORIGINAL MULTIBODY METHOD

The original method for the dynamics of multibody systems is briefly described in this Section. The modeling is carried out in dependent fully-Cartesian coordinates, also known as natural coordinates. Further explanation about these coordinates and the constraints they lead to can be found in [16].

The equations of motion of the whole multibody system are given by an index-3 augmented Lagrangian formulation in the form

$$\mathbf{M}\ddot{\mathbf{q}} + \mathbf{\Phi}_{\mathbf{q}}^{\mathrm{T}}\alpha\mathbf{\Phi} + \mathbf{\Phi}_{\mathbf{q}}^{\mathrm{T}}\boldsymbol{\lambda}^* = \mathbf{Q} \qquad (5)$$

where $\mathbf{M}$ is the mass matrix, $\ddot{\mathbf{q}}$ are the accelerations, $\mathbf{\Phi}_{\mathbf{q}}$ the Jacobian matrix of the constraint equations, α the penalty factor, $\mathbf{\Phi}$ the constraints vector, $\boldsymbol{\lambda}^*$ the Lagrange multipliers and $\mathbf{Q}$ the vector of applied and velocity dependent inertia forces. The Lagrange multipliers are obtained from the following iteration process (given by sub-index i, while sub-index n stands for the time step),

$$\boldsymbol{\lambda}_{i+1}^* = \boldsymbol{\lambda}_i^* + \alpha\mathbf{\Phi}_{i+1} \qquad i=0,1,2,... \qquad (6)$$

where the value of $\boldsymbol{\lambda}_o^*$ is taken equal to the $\boldsymbol{\lambda}^*$ obtained in the previous time step.

As integration scheme, the implicit single-step trapezoidal rule is adopted. The corresponding difference equations in velocities and accelerations are:

$$\begin{aligned}
\dot{\mathbf{q}}_{n+1} &= \frac{2}{\varDelta t}\mathbf{q}_{n+1} + \hat{\dot{\mathbf{q}}}_n \\
\ddot{\mathbf{q}}_{n+1} &= \frac{4}{\varDelta t^2}\mathbf{q}_{n+1} + \hat{\ddot{\mathbf{q}}}_n
\end{aligned} \qquad (7)$$

with,

$$\begin{aligned}
\hat{\dot{\mathbf{q}}}_n &= -\left(\frac{2}{\varDelta t}\mathbf{q}_n + \dot{\mathbf{q}}_n\right) \\
\hat{\ddot{\mathbf{q}}}_n &= -\left(\frac{4}{\varDelta t^2}\mathbf{q}_n + \frac{4}{\varDelta t}\dot{\mathbf{q}}_n + \ddot{\mathbf{q}}_n\right)
\end{aligned} \qquad (8)$$

Dynamic equilibrium can be established at time step $n+1$ by introducing the difference equations (6) and (7) into the equations of motion (4), leading to

$$\frac{4}{\varDelta t^2}\mathbf{M}\mathbf{q}_{n+1} + \mathbf{\Phi}_{\mathbf{q}\,n+1}^{\mathrm{T}}\left(\alpha\mathbf{\Phi}_{n+1} + \boldsymbol{\lambda}_{n+1}\right) - \mathbf{Q}_{n+1} + \mathbf{M}\hat{\ddot{\mathbf{q}}}_n = 0 \quad (9)$$

For numerical reasons, the scaling of Eq. (8) by a factor of $\varDelta t^2/4$ seems to be convenient, thus yielding

$$\mathbf{M}\mathbf{q}_{n+1} + \frac{\varDelta t^2}{4}\mathbf{\Phi}_{\mathbf{q}\,n+1}^{\mathrm{T}}\left(\alpha\mathbf{\Phi}_{n+1} + \boldsymbol{\lambda}_{n+1}\right) - \frac{\varDelta t^2}{4}\mathbf{Q}_{n+1} + \frac{\varDelta t^2}{4}\mathbf{M}\hat{\ddot{\mathbf{q}}}_n = 0 \ (10)$$

or, symbolically $\mathbf{f}\left(\mathbf{q}_{n+1}\right) = 0$.

In order to obtain the solution of this nonlinear system, the widely used iterative Newton-Raphson method is applied

$$\left[\frac{\partial\mathbf{f}(\mathbf{q})}{\partial\mathbf{q}}\right]_i \Delta\mathbf{q}_{i+1} = -\left[\mathbf{f}(\mathbf{q})\right]_i \qquad (11)$$

being the residual vector,

$$\left[\mathbf{f}(\mathbf{q})\right] = \frac{\varDelta t^2}{4}\left(\mathbf{M}\ddot{\mathbf{q}} + \mathbf{\Phi}_{\mathbf{q}}^{\mathrm{T}}\alpha\mathbf{\Phi} + \mathbf{\Phi}_{\mathbf{q}}^{\mathrm{T}}\boldsymbol{\lambda}^* - \mathbf{Q}\right) \qquad (12)$$

and the approximated tangent matrix,

$$\left[\frac{\partial\mathbf{f}(\mathbf{q})}{\partial\mathbf{q}}\right] = \mathbf{M} + \frac{\varDelta t}{2}\mathbf{C} + \frac{\varDelta t^2}{4}\left(\mathbf{\Phi}_{\mathbf{q}}^{\mathrm{T}}\alpha\mathbf{\Phi}_{\mathbf{q}} + \mathbf{K}\right) \qquad (13)$$

where $\mathbf{C}$ and $\mathbf{K}$ represent the contribution of damping and elastic forces of the system provided they exist.

The procedure explained above yields a set of positions $\mathbf{q}_{n+1}$ that not only satisfies the equations of motion (4), but also the constraint conditions $\mathbf{\Phi} = 0$. However, it is not expected that the corresponding sets of velocities and accelerations satisfy $\dot{\mathbf{\Phi}} = 0$ and $\ddot{\mathbf{\Phi}} = 0$, because these conditions have not been imposed in the solution process. To overcome this difficulty, velocities and accelerations are projected into their corresponding constraint manifolds. The projection leading matrix is the same tangent matrix of Eq. (12). Therefore, triangularization is avoided and projections in velocities and accelerations are carried out with just forward reductions and back substitutions.

If $\dot{\mathbf{q}}^*$ and $\ddot{\mathbf{q}}^*$ are the velocities and accelerations obtained after convergence has been achieved within the Newton-Raphson iteration, their projected counterparts $\dot{\mathbf{q}}$ and $\ddot{\mathbf{q}}$ are calculated from

$$\left[\mathbf{W} + \frac{\varDelta t^2}{4}\mathbf{\Phi}_{\mathbf{q}}^{\mathrm{T}}\alpha\mathbf{\Phi}_{\mathbf{q}}\right]\dot{\mathbf{q}} = \mathbf{W}\dot{\mathbf{q}}^* - \frac{\varDelta t^2}{4}\mathbf{\Phi}_{\mathbf{q}}^{\mathrm{T}}\alpha\mathbf{\Phi}_t \qquad (14)$$

for the velocities, and

$$\left[\mathbf{W} + \frac{\varDelta t^2}{4}\mathbf{\Phi}_{\mathbf{q}}^{\mathrm{T}}\alpha\mathbf{\Phi}_{\mathbf{q}}\right]\ddot{\mathbf{q}} = \mathbf{W}\ddot{\mathbf{q}}^* - \frac{\varDelta t^2}{4}\mathbf{\Phi}_{\mathbf{q}}^{\mathrm{T}}\alpha\left(\dot{\mathbf{\Phi}}_{\mathbf{q}}\dot{\mathbf{q}} + \dot{\mathbf{\Phi}}_t\right) \ (15)$$

for the accelerations, being,

$$\mathbf{W} = \mathbf{M} + \frac{\Delta t}{2}\mathbf{C} + \frac{\Delta t^2}{4}\mathbf{K} \qquad (16)$$

3. THE PROPOSED METHOD FOR MULTIBODY AND HYDRAULIC DYNAMICS

Now, the method described in the previous Section is extended so as to also consider the hydraulic dynamic equations. The index-3 augmented Lagrangian formulation is complemented with the pressure variation equations, leading to the following combined system of equations:

$$\mathbf{M}\ddot{\mathbf{q}} + \mathbf{\Phi}_{\mathbf{q}}^{\mathrm{T}}\alpha\mathbf{\Phi} + \mathbf{\Phi}_{\mathbf{q}}^{\mathrm{T}}\lambda^* = \mathbf{Q}(\mathbf{q},\dot{\mathbf{q}},\mathbf{p}) \\ \dot{\mathbf{p}} = \mathbf{h}(\mathbf{p},\mathbf{q},\dot{\mathbf{q}}) \qquad (17)$$

where vector $\mathbf{p}$ contains the pressures of the chambers (two for each hydraulic cylinder), and the dependency of both the applied forces vector $\mathbf{Q}$ and the function $\mathbf{h}$ with respect to positions $\mathbf{q}$, velocities $\dot{\mathbf{q}}$ and pressures $\mathbf{p}$ is explicitly indicated. The Lagrange multipliers are obtained from the same iteration process already described in the previous Section.

Again, the implicit single-step trapezoidal rule is adopted as integration scheme. The corresponding difference equations in velocities, accelerations and pressure derivatives are,

$$\dot{\mathbf{q}}_{n+1} = \frac{2}{\Delta t}\mathbf{q}_{n+1} + \hat{\dot{\mathbf{q}}}_n$$

$$\ddot{\mathbf{q}}_{n+1} = \frac{4}{\Delta t^2}\mathbf{q}_{n+1} + \hat{\ddot{\mathbf{q}}}_n \qquad (18)$$

$$\dot{\mathbf{p}}_{n+1} = \frac{2}{\Delta t}\mathbf{p}_{n+1} + \hat{\dot{\mathbf{p}}}_n$$

being,

$$\hat{\dot{\mathbf{q}}}_n = -\left(\frac{2}{\Delta t}\mathbf{q}_n + \dot{\mathbf{q}}_n\right)$$

$$\hat{\ddot{\mathbf{q}}}_n = -\left(\frac{4}{\Delta t^2}\mathbf{q}_n + \frac{4}{\Delta t}\dot{\mathbf{q}}_n + \ddot{\mathbf{q}}_n\right) \qquad (19)$$

$$\hat{\dot{\mathbf{p}}}_n = -\left(\frac{2}{\Delta t}\mathbf{p}_n + \dot{\mathbf{p}}_n\right)$$

that is, the pressure derivatives take the same integration scheme than the velocities.

If dynamic equilibrium is established at time step $n+1$ by introducing the difference equations (18-19) into the differential equations (17), the following result is obtained,

$$\frac{4}{\Delta t^2}\mathbf{M}\mathbf{q}_{n+1} + \mathbf{\Phi}_{\mathbf{q}\,n+1}^{\mathrm{T}}(\alpha\mathbf{\Phi}_{n+1} + \lambda_{n+1}) - \mathbf{Q}_{n+1} + \mathbf{M}\hat{\ddot{\mathbf{q}}}_n = 0 \quad (20)$$

$$\frac{2}{\Delta t}\mathbf{p}_{n+1} - \mathbf{h}_{n+1} + \hat{\dot{\mathbf{p}}}_n = 0 \qquad (21)$$

The scaling of Eq. (20-21) by a factor of $\Delta t^2/4$ is now performed, as it was done in the previous Section for the multibody problem, thus yielding

$$\mathbf{M}\mathbf{q}_{n+1} + \frac{\Delta t^2}{4}\mathbf{\Phi}_{\mathbf{q}\,n+1}^{\mathrm{T}}(\alpha\mathbf{\Phi}_{n+1} + \lambda_{n+1}) - \frac{\Delta t^2}{4}\mathbf{Q}_{n+1} + \frac{\Delta t^2}{4}\mathbf{M}\hat{\ddot{\mathbf{q}}}_n = 0 \quad (22)$$

$$\frac{\Delta t}{2}\mathbf{p}_{n+1} - \frac{\Delta t^2}{4}\mathbf{h}_{n+1} + \frac{\Delta t^2}{4}\hat{\dot{\mathbf{p}}}_n = 0 \qquad (23)$$

or, symbolically $\mathbf{f}(\mathbf{x}_{n+1}) = 0$, with $\mathbf{x}^{\mathrm{T}} = \{\mathbf{q}^{\mathrm{T}} \quad \mathbf{p}^{\mathrm{T}}\}$.

In order to obtain the solution of this nonlinear system, the iterative Newton-Raphson method is applied,

$$\left[\frac{\partial\mathbf{f}(\mathbf{x})}{\partial\mathbf{x}}\right]_i \Delta\mathbf{x}_{i+1} = -\left[\mathbf{f}(\mathbf{x})\right]_i \qquad (24)$$

being the residual vector,

$$\left[\mathbf{f}(\mathbf{x})\right] = \frac{\Delta t^2}{4}\left\{\begin{array}{c} \mathbf{M}\ddot{\mathbf{q}} + \mathbf{\Phi}_{\mathbf{q}}^{\mathrm{T}}\alpha\mathbf{\Phi} + \mathbf{\Phi}_{\mathbf{q}}^{\mathrm{T}}\lambda^* - \mathbf{Q} \\ \dot{\mathbf{p}} - \mathbf{h} \end{array}\right\} \qquad (25)$$

and the approximated tangent matrix $\left[\dfrac{\partial\mathbf{f}(\mathbf{x})}{\partial\mathbf{x}}\right]$,

$$\begin{bmatrix} \mathbf{M} + \frac{\Delta t}{2}\mathbf{C} + \frac{\Delta t^2}{4}(\mathbf{\Phi}_{\mathbf{q}}^{\mathrm{T}}\alpha\mathbf{\Phi}_{\mathbf{q}} + \mathbf{K}) & -\frac{\Delta t^2}{4}\frac{\partial\mathbf{Q}}{\partial\mathbf{p}} \\ -\frac{\Delta t}{2}\left(\frac{\Delta t}{2}\frac{\partial\mathbf{h}}{\partial\mathbf{q}} + \frac{\partial\mathbf{h}}{\partial\dot{\mathbf{q}}}\right) & \frac{\Delta t}{2}\left(\mathbf{I}_{np} - \frac{\Delta t}{2}\frac{\partial\mathbf{h}}{\partial\mathbf{p}}\right) \end{bmatrix} \quad (26)$$

where np is the number of elements in the vector of pressures $\mathbf{p}$, and $\mathbf{I}_{np}$ is the identity matrix of such a dimension. It must be pointed out that the tangent matrix is not symmetric any more, as it was when dealing with the multibody problem alone. This fact will negatively affect to

the efficiency, since specific solvers for symmetric matrices are faster.

Once the Newton-Raphson iteration process converges, the resulting velocities and accelerations should be projected into their respective constraint manifolds in order to achieve constraint satisfaction at velocity and acceleration levels. The projection equations are exactly the same as those presented in Eq. (14-15).

4. THE EXAMPLE

The example to test this approach is shown in Fig. 2. The solution obtained by means of the proposed formulation is confronted with those obtained through other approaches. Comparison with the approach consisting of kinematically guide the actuator will enable to assess the penalty in efficiency incurred by the unified approach. Comparison with a co-integration scheme will allow to appraise the accuracy achieved by the unified approach.
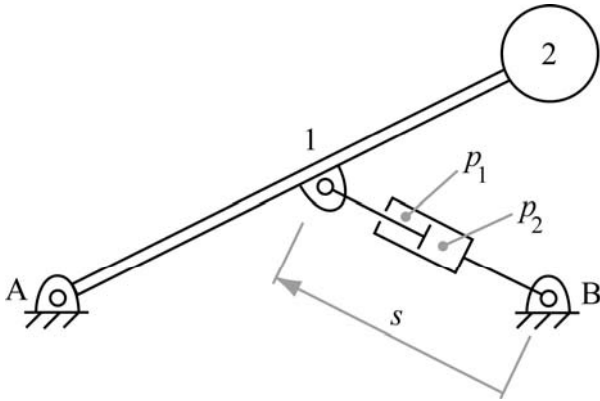
Figure 2: THE EXAMPLE.

The rod, with length L=1 m and mass m=200 kg uniformly distributed, is pinned to the ground at one of its ends in A, and has attached a point mass of M=250 kg at the other end. The system is subject to gravity. A hydraulic actuator is pinned to the center point of the rod at one end, and to the ground at the other end in B. The piston area is A=0.0065 m^2, and the total cylinder length is l=0.442 m. Friction in the actuator has been considered through a linear viscous model, with coefficient c=10^5 Ns/m. Coordinates of the fixed points are A(0,0) and B($\sqrt{3}/2$,0). Initially, the system is at rest, the angle between the rod and the ground is 30º, and the two cylinder chambers have the same volume.

The multibody system is modeled with the five variables grouped into vector $\mathbf{q}$, while the hydraulic actuator is modeled with the two pressures of vector $\mathbf{p}$,

$$\mathbf{q}^T = \{x_1 \quad y_1 \quad x_2 \quad y_2 \quad s\}$$
$$\mathbf{p}^T = \{p_1 \quad p_2\} \tag{27}$$

where x_1, y_1 are the Cartesian coordinates of point 1, located in the middle of the rod, x_2, y_2 are the Cartesian coordinates of point 2, coincident with the point mass rigidly attached to the end of the rod, s is the variable length of the hydraulic actuator, and p_1, p_2 are the pressures in the upper and lower chamber of the cylinder, respectively. The meaning of all these variables is also illustrated in Fig. 2.

According to the described data, the term of the applied forces vector $\mathbf{Q}$ of Eq. (17) due to the hydraulic actuator is,

$$\mathbf{Q}(5) = (p_2 - p_1)A - c\dot{s} \tag{28}$$

In what respects to the second set of equations in Eq. (17), i.e. the pressure equations, they are stated as follows,

$$\dot{p}_1 = h_1 = \frac{\beta_1}{Al_1}\left[A\dot{s} + A_i c_d \sqrt{\frac{2(p_P - p_1)}{\rho}}\delta_P - A_o c_d \sqrt{\frac{2(p_1 - p_T)}{\rho}}\delta_T\right]$$
$$\dot{p}_2 = h_2 = \frac{\beta_2}{Al_2}\left[-A\dot{s} + A_o c_d \sqrt{\frac{2(p_P - p_2)}{\rho}}\delta_P - A_i c_d \sqrt{\frac{2(p_2 - p_T)}{\rho}}\delta_T\right] \tag{29}$$

where β_i is calculated according to Eq. (3), l_1 and l_2 are the variable lengths of the upper and lower chamber, respectively, A_i and A_o are the variable valve areas connecting the cylinder chambers to the pump and to the tank, respectively, c_d=0.67 is the valve discharge coefficient, ρ=850 kg/m^3 is the fluid density, p_P=7.6 MPa and p_T=0.1 MPa are the pump and tank pressures, respectively (considered constant in this example), and, finally, δ_P and δ_T are 0 in case the quantity inside the square root is negative, and 1 otherwise.

Given that, as said above, the two cylinder chambers have equal volume at initial conditions, the variable lengths of the upper and lower chamber are obtained as,

$$l_1 = 0.5l + s_o - s$$
$$l_2 = 0.5l + s - s_o \tag{30}$$

with s_o=0.5 m the initial length of the actuator.

The variable valve areas A_i and A_o take, for each time instant, the following values,

$$A_i = 0.0005\kappa$$
$$A_o = 0.0005(1-\kappa) \tag{31}$$

where κ is the spool displacement or valve control parameter, i.e. the input which controls the system motion.

The initial values of the problem variables are set so that the system is in static equilibrium. This serves to avoid instabilities in the integration process. The values of the position variables, $\mathbf{q}$, are easily obtained from the initial configuration of the system described above. The initial velocities, $\dot{\mathbf{q}}$, are set to zero, since the system is at rest. The initial values of the pressures, $\mathbf{p}$, are calculated as the solution of a nonlinear system formed by the three following equations:

$$
\begin{aligned}
(2M + m)g &= (p_2 - p_1)A \\
h_1 &= 0 \\
h_2 &= 0
\end{aligned}
\tag{32}
$$

where $g=9.81$ m/s^2 is the value of gravity. The solution of the nonlinear system of Eq. (32) yields the initial values of the pressures p_1 and p_2 and the initial value of the spool displacement κ, so that static equilibrium is guaranteed.

In order to build the combined dynamic equations provided in Eq. (17), some additional terms are required. The mass matrix is,

$$
\mathbf{M} = \begin{bmatrix}
0 & 0 & 0 & 0 & 0 \\
0 & 0 & 0 & 0 & 0 \\
0 & 0 & M+\dfrac{m}{3} & 0 & 0 \\
0 & 0 & 0 & M+\dfrac{m}{3} & 0 \\
0 & 0 & 0 & 0 & 0
\end{bmatrix}
\tag{33}
$$

the applied forces are,

$$
\mathbf{Q} = \begin{Bmatrix}
0 \\
-mg \\
0 \\
-Mg \\
(p_2 - p_1)A - c\dot{s}
\end{Bmatrix}
\tag{34}
$$

and the constraints vector is,

$$
\mathbf{\Phi} = \begin{Bmatrix}
(x_1 - x_A)^2 + (y_1 - y_A)^2 - (0.5L)^2 \\
(x_2 - x_A) - 2(x_1 - x_A) \\
(y_2 - y_A) - 2(y_1 - y_A) \\
(x_1 - x_B)^2 + (y_1 - y_B)^2 - s^2
\end{Bmatrix}
\tag{35}
$$

where the first equation imposes the constant length of segment $\overline{A1}$, the second and third equations indicate that vector $\overline{A2}$ is proportional to vector $\overline{A1}$, and the fourth equation relates the variable actuator distance s with the Cartesian coordinates of points 1 and B.

Finally, in order to build the approximate tangent matrix of Eq. (26), the following terms are also required. The stiffness matrix $\mathbf{K}$ is null in this example, while the damping matrix $\mathbf{C}$ has only got the non-zero element due to the viscous damping at the actuator, $\mathbf{C}(5,5)=c$. Moreover,

$$
\begin{aligned}
\frac{\partial \mathbf{Q}}{\partial \mathbf{p}} &= A \begin{bmatrix}
0 & 0 \\
0 & 0 \\
0 & 0 \\
0 & 0 \\
-1 & 1
\end{bmatrix} \\[6pt]
\frac{\partial \mathbf{h}}{\partial \mathbf{q}} &= \begin{bmatrix}
0 & 0 & 0 & 0 & \dfrac{h_1}{l_1} \\
0 & 0 & 0 & 0 & -\dfrac{h_2}{l_2}
\end{bmatrix} \\[6pt]
\frac{\partial \mathbf{h}}{\partial \dot{\mathbf{q}}} &= \begin{bmatrix}
0 & 0 & 0 & 0 & \dfrac{\beta}{l_1} \\
0 & 0 & 0 & 0 & -\dfrac{\beta}{l_2}
\end{bmatrix} \\[6pt]
\frac{\partial \mathbf{h}}{\partial \mathbf{p}} &= -\frac{\beta c_d}{A\sqrt{2\rho}} \begin{bmatrix}
D & 0 \\
0 & E
\end{bmatrix}
\end{aligned}
\tag{36}
$$

where D and E are obtained as,

$$
\begin{aligned}
D &= \frac{1}{l_1}\left(\frac{A_i}{\sqrt{p_P - p_1}}\delta_P + \frac{A_o}{\sqrt{p_1 - p_T}}\delta_T \right) \\
E &= \frac{1}{l_2}\left(\frac{A_o}{\sqrt{p_P - p_2}}\delta_P + \frac{A_i}{\sqrt{p_2 - p_T}}\delta_T \right)
\end{aligned}
\tag{37}
$$

A 10 s maneuver is defined as the case-study: starting from rest initial conditions, the spool displacement κ is varied according to the following law:

$$\kappa = \begin{cases} \kappa_o & t \le 2 \\ \kappa_o - 0.01 & 2 < t \le 6 \\ \kappa_o + 0.01 & 6 < t \le 10 \end{cases} \qquad (38)$$

where κ_o is the initial control parameter value which provides static equilibrium conditions, as explained before.

Chronologically, the proposed unified scheme was first run, and the histories of the cylinder length s and its first and second time-derivatives were stored during the simulation.

In the second simulation executed, a program which implements the simplified approach (kinematic guidance of the actuator) was run. The histories of the cylinder length and its derivatives, stored in the previous simulation, were recovered and used to kinematically guide the coordinate s of the multibody problem, so that the same motion of the system was ensured. It must be pointed out that this second simulation is not a kinematic simulation, but a dynamic one provided by the formalism described in Section 2, in which the value of the problem variable associated to the cylinder, s, is imposed by means of an additional kinematic constraint. Therefore, the constraints vector is not that shown in Eq. (35), but the following one,

$$\Phi = \begin{Bmatrix} (x_1 - x_A)^2 + (y_1 - y_A)^2 - (0.5L)^2 \\ (x_2 - x_A) - 2(x_1 - x_A) \\ (y_2 - y_A) - 2(y_1 - y_A) \\ (x_1 - x_B)^2 + (y_1 - y_B)^2 - s^2 \\ s - s(t) \end{Bmatrix} \qquad (39)$$

Finally, a third simulation implementing a multi-rate integration scheme (different integrators and time steps) was carried out. The multibody problem conducted the integration. A time step of 10 ms was adopted for the multibody integration, while the hydraulic problem was integrated through a forward Euler integrator with a time step of 0.1 ms. These time-step sizes imply that, at every iteration of the multibody problem, the hydraulic problem must be integrated 100 times.

The integration of the hydraulic expressions given in Eq. (29) implies to assume a constant elongation velocity of the actuator during the multibody time step. This velocity is approximated by the length variation divided by the time-step size:

$$\dot{s} = \frac{s(t_{n+1}) - s(t_n)}{\Delta t} \qquad (40)$$

The Newton-Raphson scheme of the multibody integration yields, at every iteration step, a variation of the elongation at time t_{n+1}, so that a new integration of the hydraulic equations is required. Therefore, the total time of the simulation will be larger than in the case of the unified approach. However, the theoretically more accurate solution will serve to validate the solution provided by the scheme proposed in this paper.

The results obtained from the three simulations, along with their discussion, are addressed in the next Section.

5. RESULTS AND DISCUSSION

Fig. 3 shows the histories of the cylinder length, s, and its first derivative, $\dot{s}$. Fig. 4 plots the difference between the elongation, s, obtained by both the unified method and the multi-rate integration. Fig. 5 presents the histories of the pressures p_1 and p_2. The grey line provides the solutions of the multi-rate integration while the black line represents the solutions of the unified method. A detail of the discrepancies between both solutions is presented in Fig. 6.

Fig. 7 illustrates the actuator force, including the damping losses. Fig. 8 plots the histories of the total energy, the kinematic energy, the potential energy, and the work performed by the actuator (including the damping losses again). Fig. 9 gathers the violation of the constraints and their first and second derivatives (in all the three cases, the plotted magnitude is the norm of the corresponding vector).

Solutions in position, velocity and acceleration of the cylinder show practically no discrepancies between the two methods. Because of this, only one single line can be appreciated in the plots and the difference between the solution provided by multi-rate and unified integration is detailed in Fig. 4. As it can be appreciated, this difference is under 0.1 mm in the positions.

In order to validate the solution of the unified scheme, a comparison of the evolution of the pressures is depicted in Fig. 5 and a detail of the pick value of pressure p_1 is provided in Fig. 6. As explained before, the hydraulic problem is stiff, this behavior being evidenced in Fig. 6. The multi-rate scheme employs a smaller integration step for the hydraulic problem that yields a smoother solution. But, in general terms, the solution of the unified scheme is accurate and oscillations are not relevant.

It must be said that, although typical values of the penalty factor α (see Eq. (5)) are in the range 10^7-10^9, in this case a value of $\alpha = 10^{10}$ has been shown to provide the best convergence properties for the Newton-Raphson iteration of the unified scheme. The need of such a large penalty factor is due to the stiffness introduced in the system by the hydraulic equations.
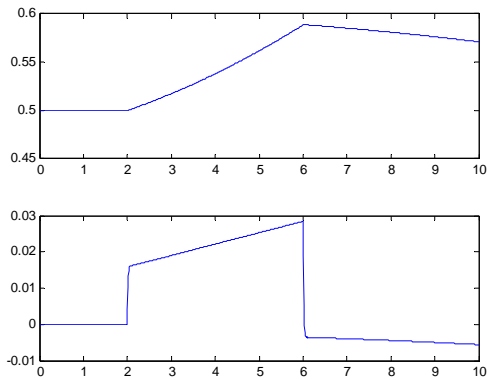
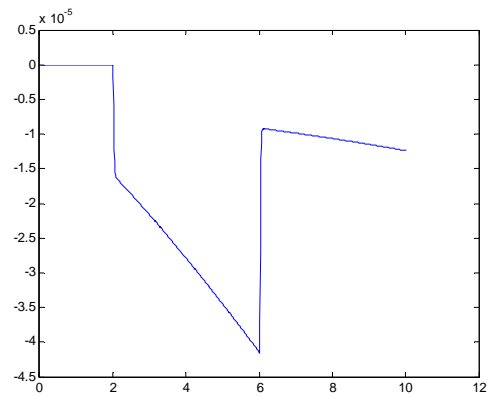Figure 3: HISTORIES OF THE CYLINDER LENGTH, s, AND ITS FIRST DERIVATIVE, $\dot{s}$.

Figure 4. DIFFERENCE BETWEEN THE HISTORIES OF THE CYLINDER ELONGATION OBTAINED BY MULTI-RATE AND UNIFIED METHOD.
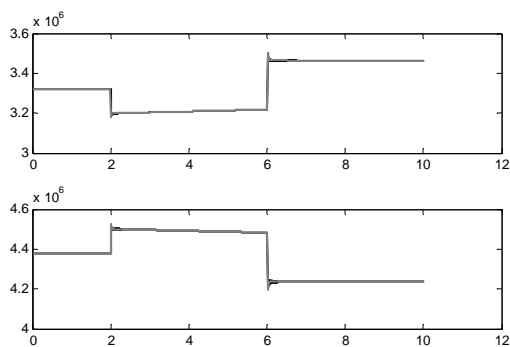

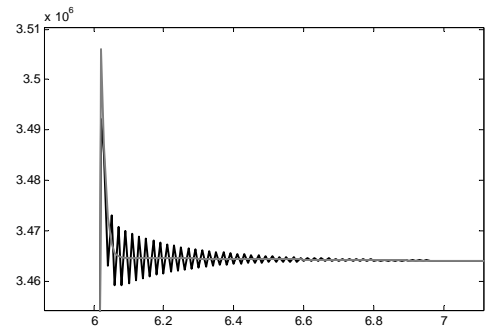Figure 5: HISTORIES OF THE PRESSURES p_1 AND p_2 .

Figure 6: DETAIL OF THE DISCREPANCIES BETWEEN p_1 VALUES OBTAINED BY MULTI-RATE (GREY) AND UNIFIED METHOD (BLACK).
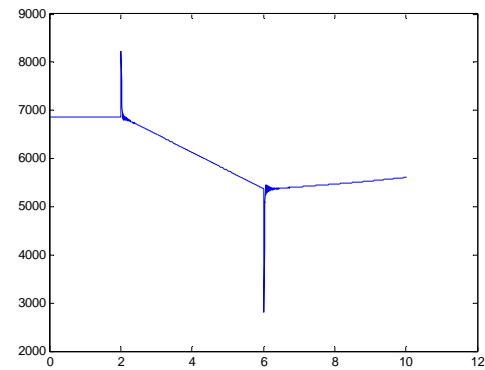

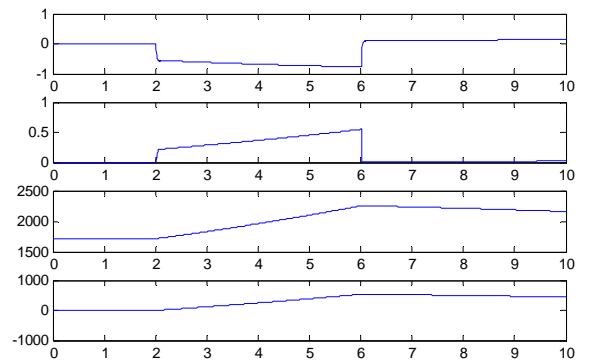Figure 7: HISTORY OF THE ACTUATOR FORCE, INCLUDING THE DAMPING LOSSES.

Figure 8: HISTORIES OF THE TOTAL, KINEMATIC AND POTENTIAL ENERGY, AND ACTUATOR WORK.
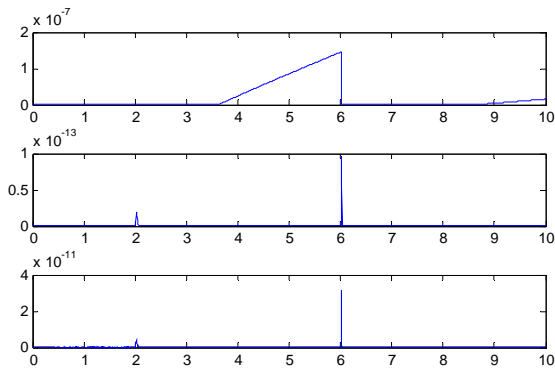
Figure 9: VIOLATION OF THE CONSTRAINTS AND THEIR FIRST
AND SECOND DERIVATIVES.

In what respects to the time-step size of integration, the plotted results have been obtained with a fixed time-step of 10 ms for the unified integration scheme, the multibody part of the multi-rate integration scheme, and the simplified simulation. Of course, smaller time-step sizes have been tested too and can be used without problem. The integration time-step size for the hydraulic problem at the multi-scale scheme has been set at 0.1 ms. Larger time steps did not reach convergence.

The number of iterations required for convergence with $\alpha=10^{10}$ and $\Delta t=10$ ms has been two or three at the more demanding instants of the simulation (around $t=2$ s and $t=6$ s) and just one for the rest. The plot of the total energy in Fig. 6 shows good conservation properties: there is a variation of 1 J in the total energy during the simulation, which is a small quantity face to variations of potential energy and actuator work of around 1000 J. The plots of constraints violation at position, velocity and acceleration levels in Fig. 7 prove that constraint satisfaction is kept within very strict limits. Therefore, the algorithm has shown a good behavior for such a large time-step size of integration, which confirms that it conserves the robustness already demonstrated in multibody simulations.

Table 1: CPU-TIMES FOR THE THREE COMPARED
APPROACHES.

Simulation	CPU-time (s)
Kinematic guidance	0.338
Unified integration	0.389
Multi-rate integration	11.634

Regarding the efficiency, CPU-times measured for the three simulations performed are shown in Table 1. The programs were developed and run in Matlab computing environment, which means that absolute CPU-times are not representative, yet they serve for comparison among the different approaches.

In Table 1, the increase in computational cost motivated by the inclusion of the hydraulic equations in the unified scheme is around 20% with respect to the simplified simulation, that only considers the multibody problem. From the theoretical point of view, the increase in computational cost is basically due to two factors: on the one hand, to the larger problem size, since the pressures are added to the problem variables, and, on the other hand, to the non-symmetric character of the new approximated tangent matrix of the Newton-Raphson iteration.

The comparison between the unified scheme and multi-rate approach is very favorable to the unified scheme. Multi-rate integration with the mentioned time-step sizes implies to evaluate and integrate the hydraulic equations 100 times at every iteration within a time step of the multibody integration. The use of a more stable integrator for the hydraulic problem might lead to a smaller difference between both methods, but the obtained results highlight the fact that the smaller step size of the hydraulic problem notably slows down the integration.

Evidently, these trends require further confirmation in the simulation of large and complex machines, like for example the full model of an excavator, but the analysts interested in moving from the simplified or multi-rate integration to the unified approach may have this study into account.

6. CONCLUSIONS
At the view of the results, the following conclusions can be established:
- The augmented Lagrangian formulation traditionally used to address multibody dynamics problems conserves its robustness when facing combined multibody and hydraulic dynamics problems in a unified approach. For the academic example studied, a large time-step size of 10 ms could be taken, but a high penalty factor of 10^{10} was required in order to keep good convergence properties, due to the stiffness of the hydraulic equations.
- The increase in computational cost motivated by the inclusion of the hydraulic equations when compared with a simplified modeling of the hydraulic problem through kinematic guidance of the actuators is moderated, and due mainly to the larger resulting problem size and the non-symmetric character of the approximated tangent matrix. A 20% increase was measured for the academic example considered. Therefore, it can be affirmed that the efficiency is not

substantially altered when moving from a simplified to a fully-coupled approach.

- The unified approach is largely more efficient than the multi-rate integration scheme due to the lower number of evaluations of the hydraulic equations required. However, discrepancies between the solutions provided by both methods are not relevant.

7. ACKNOWLEDGMENT

REFERENCES

1. Cuadrado J., Cardenal J., Morer P., Bayo E., Intelligent Simulation of Multibody Dynamics: Space-State and Descriptor Methods in Sequential and Parallel Computing Environments, *Multibody System Dynamics*, Vol. 4, pp. 55-73, 2000.
2. Cuadrado J., Dopico D., Gonzalez M., Naya M.A., A Combined Penalty and Recursive Real-Time Formulation for Multibody Dynamics, *Journal of Mechanical Design*, Vol. 126, pp. 602-608, 2004.
3. Fales R., Spencer E., Chipperfield K., Wagner F., Kelkar A., Modeling and Control of a Wheel Loader with a Human-in-the-Loop Assessment using Virtual Reality, *Journal of Dynamic Systems, Measurement, and Control*, Vol. 127, pp. 415-423, 2005.
4. Sekhavat P., Sepehri N., Wu Q., Impact Stabilizing Controller for Hydraulic Actuators with Friction: Theory and Experiments, *Control Engineering Practice*, Vol. 14, pp. 1423-1433, 2005.
5. Merritt H.E., *Hydraulic Control Systems*, Wiley, New York, 1967.
6. Eryilmaz B., Wilson B.H., Unified Modeling and Analysis of a Proportional Valve, *Journal of the Franklin Institute*, Vol. 343, pp. 48-68, 2006.
7. Gonzalez M., Luaces A., Dopico D., Cuadrado J., A 3D Physics-Based Hydraulic Excavator Simulator, *Proceedings of the ASME World Conference on Innovative Virtual Reality (WINVR09)*, Paper 734, Chalon-sur-Saone, France, 2009.
8. Vaculin M., Valasek M., Krüger W.R., Overview of Coupling of Multibody and Control Engineering Tools, *Vehicle System Dynamics*, Vol. 41, pp. 415-429, 2004.
9. Valasek M., Modeling, Simulation and Control of Mechatronical Systems, *Simulation Techniques for Applied Dynamics (Arnold M. and Schiehlen W. eds.)*, Springer, Wien-New York, 2008.
10. Brüls O., Arnold M., The Generalized-α Scheme as a Linear Multistep Integrator: Towards a General Mechatronic Simulator, *Proceedings of the ASME Int. DETC & CIEC*, Las Vegas, Nevada, USA, 2007.
11 Pfeiffer F., Foerg M., and Ulbrich H., Numerical Aspects of Non-Smooth Multibody Dynamics. *Computer Methods in Applied Mechanics and Engineering*, Vol. 195, pp. 6891-6908, 2006.
12. Busch M., Arnold M., Heckmann A., Dronka S., Interfacing SIMPACK to Modelica/Dymola for Multi-Domain Vehicle System Simulations, *SIMPACK News*, Vol. 11, No. 2, pp. 1-3, 2007.
13. Cardona A. and Geradin M., Modeling of a Hydraulic Actuator in Flexible Machine Dynamics Simulation, *Mechanisms and Machine Theory*, Vol. 25, pp. 193-207, 1990.
14. Bauchau O.A. and Liu H., On the Modeling of Hydraulic Components in Rotorcraft Systems, *Journal of the American Helicopter Society*, Vol. 51, pp. 175-184, 2006.
15. Welsh W.A., Simulation and Correlation of a Helicopter Air-Oil Strut Dynamic Response, *Proceedings of the American Helicopter Society 43rd Annual Forum*, St. Louis, Missouri, USA, 1987.
16. Garcia de Jalon J., Bayo E., *Kinematic and Dynamic Simulation of Multibody Systems –The Real-Time Challenge–*, Springer-Verlag, New York, 1994.